Available online at www.eccomasproceedia.org
Eccomas Proceedia COMPDYN (2025) 577 -5780

ECCOMAS
Proceedia

COMPDYN 2025
10th ECCOMAS Thematic Conference on
Computational Methods in Structural Dynamics and Earthquake Engineering
M. Papadrakakis, M. Fragiadakis (eds.)
Rhodes Island, Greece, 15-18 June 2025

AXIAL LOAD RATIO (ALR) LIMIT OF THE SLENDER FLANGED RC SHEAR WALLS WITH HIGH-STRENGTH REBAR

Nilanjan. Samanta[1], **Kaustubh. Dasgupta**[2], **and Luigi. Di Sarno**[3,4]

[1] Department of Civil engineering
Indian Institute of Technology Guwahati, India
e-mail: nsamanta@iitg.ac.in

[2] Department of Civil Engineering and Center for Disaster Management and Research
Indian Institute of Technology Guwahati, India
e-mail: kd@iitg.ac.in

[3]Department of Civil and Environmental Engineering
University of Liverpool
Liverpool, UK
e-mail: luigi.di-sarno@liverpool.ac.uk

[4]Department of Structures for Engineering and Architecture
University of Naples Federico II
Naples, Italy
e-mail: disarno@unina.it

Abstract

In the RC wall-frame (dual) system, the RC structural wall acts as the primary lateral load-resisting component, increasing the global stiffness, strength, and ductility of the building. In tall buildings, RC shear walls are subjected to higher axial load ratios (ALRs), which greatly impair the displacement ductility and collapse drift capacity of RC structural walls. Failure modes of slender RC shear walls are very sensitive to the ALR. Various international standards and codes have prescribed the upper limit of the ALR for rectangular RC structural walls to address the adverse effect of the higher compressive forces. It is to be noted that none of these codes or standards have exclusively mentioned the ALR limit for flanged slender RC structural walls. In the current study, the upper limit of the ALR is proposed for flanged RC structural walls based on the nonlinear static behaviour of the three-dimensional finite element (FE) model. Building on past research, the parameters that influence ultimate drift, yield drift, and displacement ductility are identified. Such parameters are then investigated to determine their influence on yield drift, collapse drift, and displacement ductility capacities within the typical ALR range of 0 to 0.2. Finally, based on the mean values of displacement ductility capacity and the collapse drift, a design recommendation of ALR for flanged shear walls is provided.

Keywords: Flanged shear wall, Axial load ratio, Collapse drift, Displacement ductility.

ISSN:2623-3347
doi: 10.7712/120125.12848.25865

1 INTRODUCTION

Slender Reinforced Concrete (RC) shear walls in tall buildings frequently experience substantial compressive forces during strong earthquake shaking. This is often a result of architectural designs aimed at maximizing floor-to-ceiling heights and usable space. A previous study [1] had shown that structural wall elements in highrise buildings can withstand Axial Load Ratio (ALR) up to 0.4. This value exceeds the typical range of 0 to 0.2. Past experimental studies [2,3] have proved that the high ALR (above 0.3) severely impairs the displacement ductility and collapse drift capacity of RC shear walls. Hence, these walls experience rapid stiffness and strength degradation and finally fail in a brittle way when subjected to reverse slow cyclic load under higher ALR. The 2010 Chile earthquake provided valuable insights into the impact of high ALR on the seismic behavior of RC structural walls. Post-earthquake investigations revealed that thinner walls, typically 150 mm to 200 mm thick, in newer highrise structures experienced greater damage than the thicker walls found in older buildings, likely due to higher ALR. Under low ALR, the failure mode of such a wall is either fracture of tensile rebar or crushing of concrete in the compression zone at a larger lateral drift which ensures ductile behaviour. Whereas, under high ALR, crushing of concrete in the compression zone of the wall is followed by buckling of longitudinal rebar at a very early stage which results in a very brittle behavior at the global level. In the present study, a threshold value for the upper limit of ALRs is suggested for the flanged RC structural wall based on the nonlinear static response of the three-dimensional, FE model developed in the ABAQUS 6.14 [4] computer platform. The developed numerical model has been validated with past experimental studies. The primary parameters influencing ultimate drift, yield drift, and displacement ductility of flanged RC structural walls are identified based on previous studies. A parametric study is conducted to determine the influence of the considered parameters on the collapse drift, yield drift, displacement ductility capacity, and peak lateral shear capacity. Finally, based on the average values of displacement ductility capacity and collapse drift level, a design recommendation of ALR is suggested for flanged RC structural walls.

2 OBJECTIVE AND RELEVANCE OF THE STUDY

In tall buildings, RC shear walls are subjected to higher axial compressive force which impairs the displacement ductility capacity and collapse drift capacity of RC structural walls to a large extent. In the case of flanged RC structural walls, the participation of the flange reduces both the displacement ductility capacity and the ultimate drift capacity, as compared to rectangular RC structural walls [5]. Moreover, the use of high-strength rebar in flanged RC structural walls further reduces displacement ductility capacity due to the amplification of yield drift. The present standards [6-10] have suggested the upper limit of ALR for rectangular RC structural walls exclusively but no such prescription exists for flanged RC structural walls. This numerical study proposes the upper limit of the ALR for flanged RC structural walls (satisfying the minimum thickness criteria of Indian standards [11]) built with high-strength rebar based on the specified limits for minimum collapse drift and displacement ductility capacity. The suggested recommendation of ALR is expected to further assist practical designers in fixing the cross-sectional sizes of flanged RC shear walls.

3 RECOMMENDATIONS OF INTERNATIONAL STANDARDS

US standard for seismic evaluation and retrofit of buildings, ASCE/SEI 41-17 [6] has explicitly mentioned that structural RC walls with axial compressive load > $0.35P_o$, where, P_o represents the nominal axial strength, should not be considered to be effective for resisting earthquake forces. Canadian concrete design code [7] stipulates that the flexural members having factored axial compressive force $P_u > 0.35P_o$, should not be used for earthquake resistance. New Zealand Concrete Design Code NZS 3101 [11] does not prescribe explicitly any ALR limit but it has limited the sectional curvature or material strain at the potential plastic hinge locations in the shear wall. Seismic Design Standards such as Eurocode 8 [8], GB 50011-2010 [9], and HK-CP 2013 [10] have explicitly mentioned the ALR limit for RC structural walls. It is worth mentioning that none of these codes or standards has exclusively suggested any ALR limit for slender flanged RC structural walls. In the present study, ALR (η) is defined as:

$$\eta = \frac{P_u}{f_{ck}A_g} \tag{1}$$

Where P_u is the factored axial compressive force, f_{ck} is the characteristic cube compressive strength of concrete and A_g is the gross cross-sectional area of concrete. Similarly, in the current study, the peak shear strength, v_n (lateral load capacity) is normalised as:

$$v_n = \frac{V_{max}}{A_w\sqrt{f_{ck}}} \tag{2}$$

Where V_{max} is the maximum lateral load capacity and A_w is the web area of the T-shaped RC wall.

4 PRESCRIBED ULTIMATE DRIFT AND DISPLACEMENT DUCTILITY

While Indian Standards do not specify a minimum ultimate drift capacity or displacement ductility capacity for RC structural walls, many International Standards define such limits. Eurocode 8 [8] has prescribed the limit of interstorey drift requirement for RC buildings as 1% at the ultimate limit state. Similarly, GB 50011 [9] has prescribed the elastoplastic storey drift requirements for the RC structural wall and RC frame-wall as 0.83% and 1%, respectively. AS 1170.4 [13] has stipulated that the interstorey drift requirement for RC buildings at the ultimate limit state as 1.5%. NBCC-15 [14] has specified that the interstorey drift requirement for RC buildings at the ultimate limit state as 2.5%. A past experimental study [15] on flanged RC structural walls has confirmed that the stipulation given by NBCC-15 and AS 1170.4 overestimates the collapse drift capacity of flanged RC structural walls. In contrast, the values prescribed by Eurocode 8 and GB 50011 are more realistic. In the current study, the limit of interstorey drift prescribed by GB 50011 and Eurocode 8, *i.e.*, 1% interstorey drift is considered as the ultimate or collapse drift limit. It is to be noted here that along with satisfying the minimum collapse drift capacity, structural elements need to maintain the minimum ductility capacity. NZS 1170.5 [16] has stipulated that the Structural Ductility Factor (μ) of ductile structures (DS) should be between 3 to 6. Apart from that, AS 1170.4 has also prescribed that the minimum value of μ for ductile shear wall should be 3. In this study, for fixing the limit of ALR, the minimum Structural Ductility Factor or displacement ductility (μ) is considered as 3.

5 NUMERICAL MODEL AND ITS VALIDATION

Numerical analysis is one kind of method that helps to get a holistic insight into comprehensive structural behavior with realistic output requests. In the current study, the numerical model is developed for nonlinear analysis using ABAQUS 6.14 [4]. Ni and Lu [17] investigated the seismic behavior of the T-shaped RC structural wall (designated as T-0.1 F) built with high-strength reinforcement using quasi-static reverse cyclic loading. The same is adopted in the present study to validate the FE modelling strategy. The constitutive model of concrete is defined according to the Concrete Damage Plasticity (CDP) model which is a plasticity-based continuum damage model. The response of unconfined concrete under uniaxial compression (Figure 1(a)) is taken as per the Karthik and Mander [18] model whereas the uniaxial tensile response (Figure 1(b)) of the concrete is taken as per Wahalathantri et al. [19] model. For rebar, the experimental stress-strain response [16] for two grades of steels, namely HRB_400MPa and HRB_600MPa, are considered in the study (Figure 1(c)).

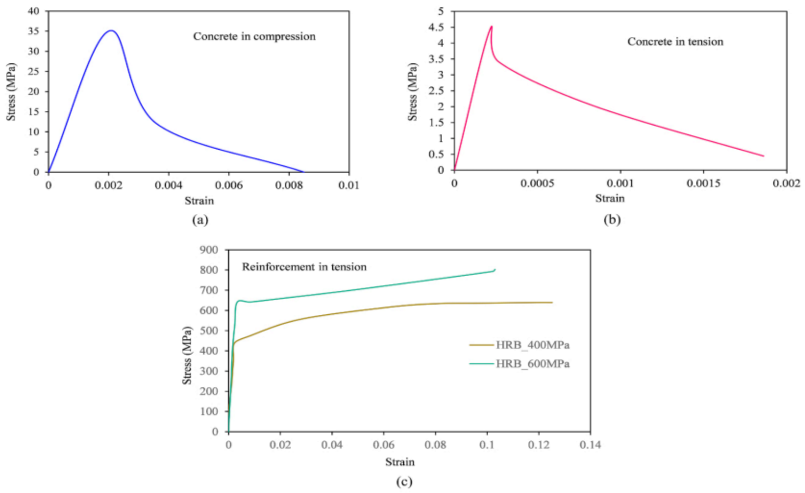

Figure 1: Stress-strain relationships for (a) concrete in uniaxial compression, (b) concrete in uniaxial tension, and (c) steel reinforcement.

Concrete elements are modeled as eight-node solid linear brick elements having reduced integration with hourglass control (C3D8R) from the ABAQUS/Standard element library. Reinforcement bars are modeled as wire features integrated with the two-node 3D linear truss element (T3D2). The rebars are considered to be embedded in the concrete by using the *Embedded Element Constraints* which ensures strain compatibility of reinforcement with adjacent concrete. In the current study, the loading is applied in two phases. In the first phase, the self-weight and external axial load is applied and in the second phase, the monotonic load is given in a displacement-controlled manner. Although reverse cyclic displacement-based analysis predicts a more realistic response of the wall, monotonic displacement-based analysis is adopted in the present study due to resource constraints. Finally, the monotonic lateral load – lateral drift relationship is compared with the backbone curve of the experimental lateral load – lateral drift relationship of T-0.1 F which is shown in Figure 2.

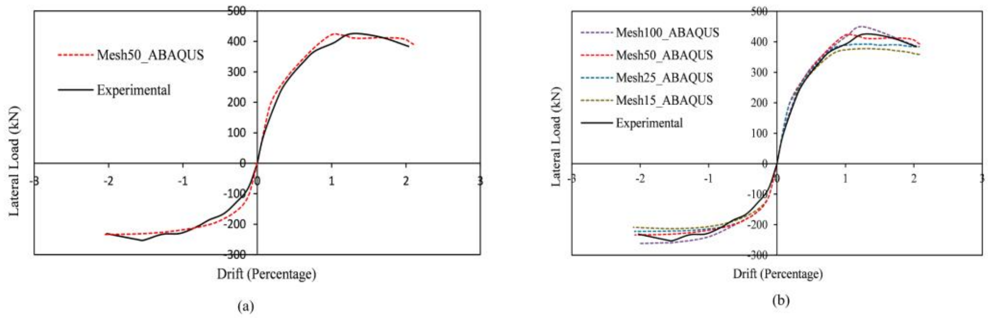

Figure 2: Lateral load-drift relationship for T-0.1 F: (a) comparison of numerical result and the experimental result, and (b) mesh sensitivity study

A mesh sensitivity study is also carried out and the optimum size of the mesh is found to be 50 mm with an aspect ratio of 1.

6 PARAMETRIC STUDY FOR FIXING THE LIMIT OF ALR

Previous studies [20, 21] have shown that certain parameters significantly influence yield drift, ultimate drift, and consequently, the displacement ductility capacity. In the current study, the parameters that are adopted for finding out the upper limit of ALR are given in Table 1. In the present study, three values of ALR are chosen. Two (η = 0 and η = 0.1) of them are lower than the ratio required for a balanced condition and one (η = 0.2) is higher than the ratio required for a balanced condition. It is worth mentioning here that unless otherwise specified, the parametric study with zero ALR invariably means that only the self-weight of the structural wall is considered. In this study, the aspect ratio of the numerical model for the T-shaped RC wall has been taken as 2.1 to ensure the occurrence of flexure-dominant failure mode. Although the FE model for the T-shaped RC wall has been validated for both web parallel flange-in-tension and web parallel flange-in-compression bending modes, in the current study, only the web parallel flange-in-tension bending mode is considered here as under this mode, T-shaped RC wall is expected to exhibit lowest collapse drift and displacement ductility capacity. This phenomenon can also be confirmed by the large neutral axis depth and the participation of the flange for the web parallel flange-in-tension bending mode. It is to be noted that in the present study, the ultimate or collapse drift is determined as per the recommendation of Kazaz et al. [21] whereas the yield drift is determined as per the proposal of Park [22].

Parameter	Value
Axial load ratio (η)	0, 0.1, 0.2
Web boundary longitudinal reinforcement ratio (ρ)	1.2%, 2.2%, 3%
Web transverse reinforcement ratio (ρ_h)	0.25%, 0.5%
Flange width-to-wall length ratio (b_f/l_w)	0.7, 1, 1.3

Table 1: Summary of the parameters considered

7 RESULTS AND DISCUSSION

This section presents the influence of ALR on yield drift, ultimate or collapse drift, displacement ductility, and peak lateral shear strength for different parameters, such as the web boundary longitudinal reinforcement ratios (ρ), the web transverse reinforcement ratios (ρ_h), and the flange length-to-wall length ratios (b_f/l_w). For all the considered parameters, the influence of ALR on the yield drift, ultimate drift, ductility, and peak shear strength (peak lateral load capacity) of the T-shaped RC wall is plotted in Figure 3. From Figure 3(a), it is evident that displacement ductility decreases with increasing ALR due to shifting down of the Neutral axis (NA) under higher ALR. With the increase in ALR, the normalised peak lateral shear capacity (lateral load capacity) always increases due to the corresponding increase in the moment of resistance of the wall section (Figure 3(b)). For both under-reinforced and over-reinforced wall sections, the NA shifts down with increasing ALR, causing a reduction in the ultimate drift capacity (Figure 3(c)). For under-reinforced sections, the yield drift capacity tends to increase with ALR due to an increase in the depth of NA (η = 0 and η = 0.1) (Figure 3(d)). On the other hand, for the over-reinforced section (η = 0.2), yield drift capacity decreases due to the shifting down of NA.

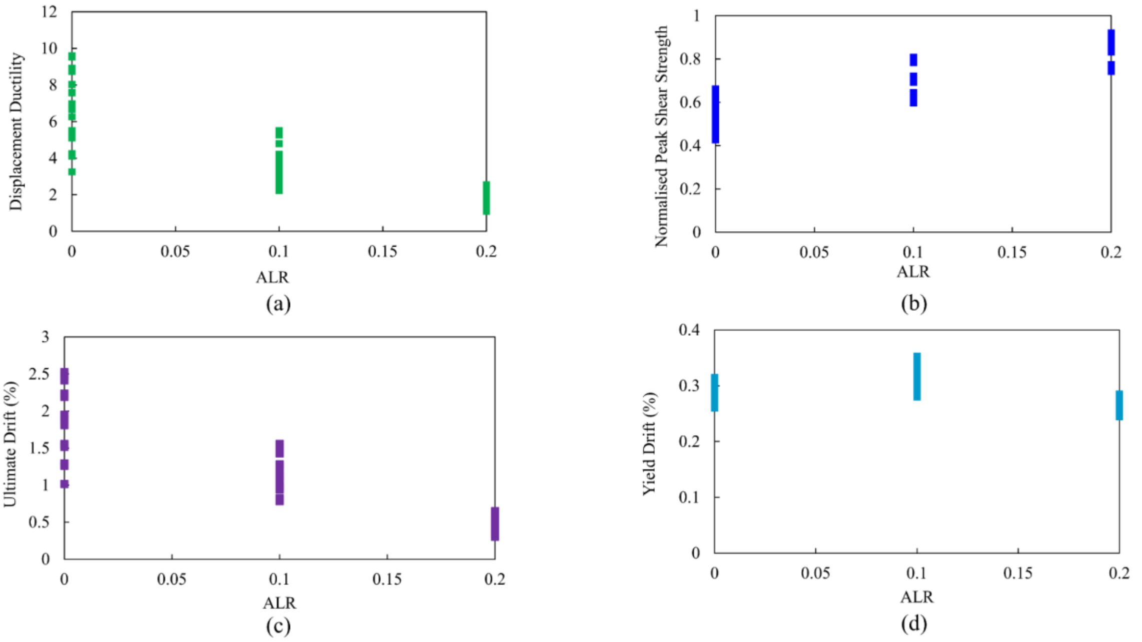

Figure 3: Influence of ALR on (a) displacement ductility capacity, (b) normalised peak shear strength, (c) ultimate drift capacity, and (d) yield drift capacity

8 DESIGN RECOMMENDATION ON ALR LIMIT

Figure 4 presents the variation of average ultimate drift capacity and displacement ductility capacity for the considered range of ALRs. It is evident that as the ALR increases, ultimate drift (Figure 4(a)) and displacement ductility capacity (Figure 4(b)) show a decreasing trend. The results indicate that based on the minimum ultimate drift capacity (say 1%) as well as the minimum structural ductility factor (say 3), the upper limit of ALR can be taken as 0.1.

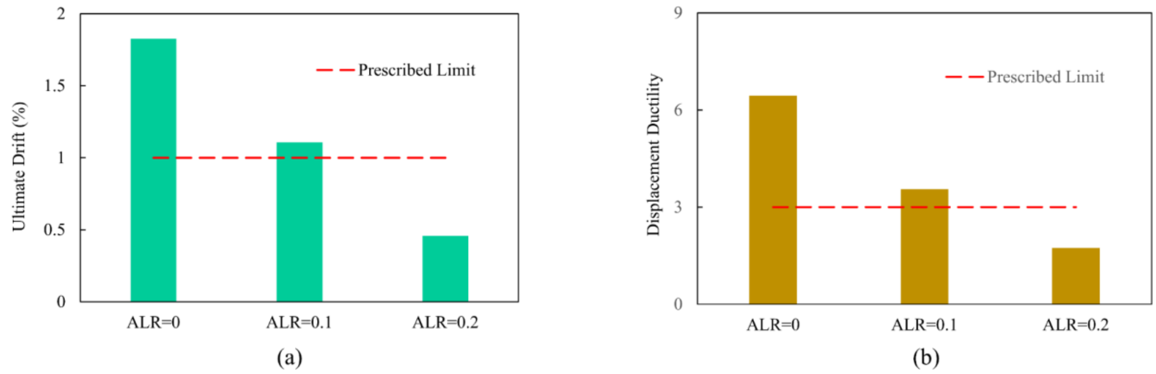

Figure 4: Variation of (a) mean ultimate drift capacity and (b) mean displacement ductility, with ALR

9 CONCLUSIONS

The following salient conclusions can be drawn from the present study:

- As ALR increases, displacement ductility and ultimate drift capacities exhibit a monotonically decreasing trend due to the downward shift of the neutral axis.
- It is evident that with the increase in ALR with a certain limit, the lateral load capacity of flanged RC shear walls tends to increase.
- With the increase in ALR, yield drift capacity tends to increase for the under-reinforced section, whereas, for the over-reinforced section, it tends to reduce.
- Finally, the upper limit of ALR for slender flanged RC structural walls is proposed as 0.1 for satisfying the minimum ultimate drift capacity and the structural ductility factor. This will help the designer to fix the cross-sectional sizes of such walls for better earthquake-resistant behaviour.

REFERENCES

[1] J. W. Wallace, L. M. Massone, P. Bonelli, J. Dragovich, R. Lagos, C. Lüders, J. Moehle, Damage and implications for seismic design of RC structural wall buildings. *Earthquake Spectra*, 28, 281-299, 2012.

[2] R. K. L. Su, S. M. Wong, Seismic behaviour of slender reinforced concrete shear walls under high axial load ratio. *Engineering Structures*, 29, 1957-1965, 2007.

[3] Y. Zhang, Z. Wang, Seismic behavior of reinforced concrete shear walls subjected to high axial loading. *ACI Structural Journal*, 97, 739-750, 2000.

[4] ABAQUS, 2014. Version 6.14 User's Manual, Dassault Systèmes Simulia Corp.; Providence, RI, USA.

[5] X. Ni, S. Cao, H. Aoude, Seismic performance of concrete walls reinforced by high-strength bars: cyclic loading test and numerical simulation. *Canadian Journal of Civil Engineering*, 48, 1481-1495, 2021.

[6] American Society of Civil Engineers (ASCE). ASCE/SEI 41-17: Seismic evaluation and retrofit of existing buildings. Reston, Varginia, USA; 2017.

[7] CSA-A23.3-04 (R2010). Design of concrete structures. Rexdale, Ontario: Canadian Standard Association;2010.

[8] Eurocode 8. Design of structures for earthquake resistance – Part 1: General rules, seismic actions, and rules for buildings. The European Standard EN; 2004.

[9] GB50011-2010. Code for seismic design of building. China Ministry of Construction, Beijing (China); 2010 [in Chinese].

[10] HK CP 2013. Code of practice for structural use of concrete. Building Department, Mongkok, Kowloon, Hong Kong; 2013.

[11] Bureau of Indian Standards (BIS). Ductile design and detailing of reinforced concrete structures subjected to seismic forces—Code of practice, IS 13920. New Delhi, India; 2016.

[12] NZS 3101. The design of concrete structures. New Zealand: Standards New Zealand; 2006.

[13] AS 1170.4. Structural design actions - part 4: earthquake actions in Australia. Sydney, Australia: Standards Australia; 2007.

[14] National Building Code of Canada (NBCC). Institute for Research in Construction. Ottawa, Ontario, Canada: National Research Council of Canada; 2015.

[15] B. Wang, M. Z. Wu, Q. X. Shi, W. Z. Cai, Seismic performance of flanged RC walls under biaxial cyclic loading. Journal of Building Engineering, 64, 105632, 2023.

[16] NZS 1170.5. Structural Design Actions. Wellington, New Zealand: Standard New Zealand; 2004.

[17] X. Ni, N. Lu, Cyclic tests on T-shaped concrete walls built with high-strength reinforcement. *Journal of Earthquake Engineering*, 26, 5721-5746, 2022.

[18] M. M. Karthik, J. B. Mander, Stress-block parameters for unconfined and confined concrete based on a unified stress-strain model. *Journal of Structural Engineering*, 137, 270-273, 2011.

[19] B. Wahalathantri, D. Thambiratnam, T. Chan, S. Fawzia (2011). A material model for flexural crack simulation in reinforced concrete elements using ABAQUS. *In Proceedings of the first international conference on engineering, designing and developing the built environment for sustainable wellbeing*, Queensland University of Technology, 2011.

[20] M. J. N. Priestley, M. J. Kowalsky, Aspects of drift and ductility capacity of rectangular cantilever structural walls. *Bulletin of the New Zealand Society for Earthquake Engineering*, 31, 73-85, 1998.

[21] İ. Kazaz, P. Gülkan, A. Yakut, Deformation limits for structural walls with confined boundaries. *Earthquake Spectra*, 28(3), 1019-1046, 2012.

[22] R. Park, Evaluation of ductility of structures and structural assemblages from laboratory testing. *Bulletin of the New Zealand Society for Earthquake Engineering*, 22, 155-166, 1989.